Inorganic Chemistry

pubs.acs.org/IC

Article

Programmable Nuclear-Spin Dynamics in Ti(IV) Coordination Complexes

Spencer H. Johnson, Cassidy E. Jackson, and Joseph M. Zadrozny*

Cite This: https://dx.doi.org/10.1021/acs.inorgchem.0c00244

Read Online

ACCESS | Metrics & More | Article Recommendations | Supporting Information

ABSTRACT: Interstitial patterning of nuclear spins is a nascent design principle for controlling electron spin superposition lifetimes in open-shell complexes and solid-state defects. Herein we report the first test of the impact of the patterning principle on ligand-based nuclear spin dynamics. We test how substitutional patterning of ^{1}H and $^{79/81}$Br nuclear spins on ligands modulates proton nuclear spin dynamics in the ligand shell of metal complexes. To do so, we studied the ^{1}H nuclear magnetic resonance relaxation times (T_1 and T_2) of a series of eight polybrominated catechol ligands and six complexes formed by coordination of the ligands to a Ti(IV) ion. These studies reveal that ^{1}H T_1 values can be enhanced in the individual ligands by a factor of 4 (from 10.8(3) to 43(5) s) as a function of substitution pattern, reaching the maximum value for 3,4,6-tribromocatechol. The T_2 for ^{1}H is also enhanced by a factor of 4, varying by ∼14 s across the series. When complexed, the impact of the patterning design strategy on nuclear spin dynamics is amplified and ^{1}H T_1 and T_2 values vary by over an order of magnitude. Importantly, the general trends observed in the ligands also match those when complexed. Hence, these results demonstrate a new design principle to control ^{1}H spin dynamics in metal complexes through pattern-based design strategies in the ligand shell.

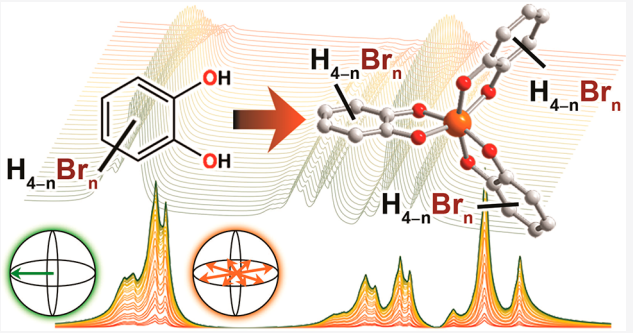

INTRODUCTION

Next-generation applications of open shell magnetic complexes rely on long-lived electronic spin superposition lifetimes. Applications for sustained molecule-based spin superpositions span quantum sensing,[1,2] quantum computation,[3,4] and dynamic nuclear polarization.[5] Toward utility in these applications, chemical design principles for lengthening superposition lifetime are critically important.[6−11] However, the realization of useful lifetimes (>100 μs) in molecules are still only achieved in environments engineered to be free of a spin bath, in terms of both nuclear and electronic spins.[12,13] Special environments like these are disjoint from applications, wherein highly active local spin environments are likely to be present. Hence, testing new design strategies to prolong spin superposition lifetime in dynamic magnetic surroundings is a pressing concern.

One prominent origin of short-lived spin superpositions in open-shell molecules is the dynamic nuclear spin bath.[14] Rapid and numerous fluctuations in the orientations of these nuclear spins, when close to an electronic spin, impose a fluctuating local magnetic field on the electron, which accelerates the collapse of electronic spin superpositions. The extent to which environmental nuclear spins impart this fluctuating local field depends on their respective nuclear relaxation dynamics. In turn, these dynamics stem (in part) from the respective interactions between the nuclear spins.[15−18] Hence, controlling the spin−spin interactions between bath nuclear spins may be a powerful method for manipulating the dynamic field and producing long-lived molecular electronic spin superpositions.

In this context, a set of chemical design principles to tune the magnetic environment imposed by the nuclei in a molecule would be extremely useful. Here, manipulation of the impact of this proximate "edge" of the larger nuclear spin bath could be achieved via synthetic modification of interspin distances, relative arrangements, and identity of nuclear spins on the molecule itself. Indeed, recent breakthroughs from our group on V(IV) complexes[19] and others on the solid-state defects in SiC[20−22] provide preliminary demonstrations of manipulating nuclear spin position/arrangements to control nearby electronic spin superpositions. Extensive literature exists on the fundamental mechanisms governing nuclear spin relaxation,[15−18] providing a foundational backbone for translating the aforementioned breakthroughs into broadly applicable design principles. Yet, generalizable synthetic strategies to tailor nuclear spin relaxation in the ligand shell of metal complexes are still absent.

Received: January 23, 2020

https://dx.doi.org/10.1021/acs.inorgchem.0c00244
Inorg. Chem. XXXX, XXX, XXX−XXX

Toward that knowledge, we herein test the dependence of ^{1}H nuclear-spin dynamics on substitutional patterning in a series of brominated catechol derivatives and upon coordination to Ti(IV) (Figure 1). We hypothesized that different

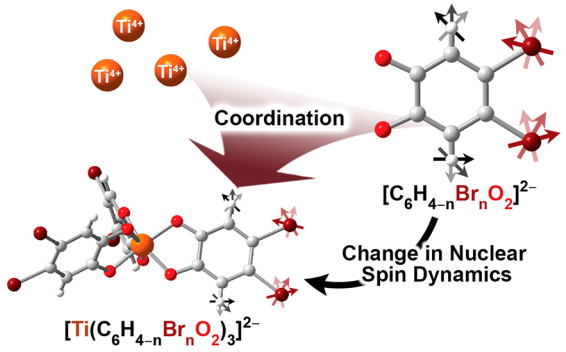

Figure 1. In this manuscript, we perform the first tests of how different substitutional patterns of ^{1}H and $^{79/81}$Br nuclear spins on ligands impact the ligand ^{1}H T_1 and T_2 and how the effect changes upon coordination.

patterns of Br functional groups on the ligand would enable a significant synthetic variation in ^{1}H spin dynamics in the isolated catechols, as bromine and hydrogen have significantly different nuclear magnetic moments (^{1}H, μ = 2.79 μ_N, ^{79}Br, μ = 2.11 μ_N, ^{81}Br, μ = 2.27 μ_N) and Larmor frequencies (at 9.4 T, ^{1}H = 400 MHz, ^{79}Br = 101 MHz, ^{81}Br = 108 MHz). We thus reasoned that different substitutional patterns on the ligand shell would modulate the interspin dipole−dipole interactions, thereby impacting T_1 and T_2.[23] The difference in Larmor frequencies was also viewed as particularly advantageous for suppressing the impact of nuclear Overhauser effects on relaxation and simplifying the analysis.[24] Finally, we predicted that these trends would be reproduced when the ligands were part of the coordination shell. This last prediction is on the basis of the distance dependence of the dipolar interactions between nuclei, which weaken with r^{-6} (where r is the distance separating nuclei).[37−39] Hence, we envisioned that interligand interactions would be minimal relative to intraligand interactions.

To test the foregoing hypotheses, we investigated the ^{1}H spin−lattice relaxation (T_1) and spin−spin relaxation (T_2) times for eight catechol molecules: pyrocatechol (**1**), 3-bromocatechol (**2**), 4-bromocatechol (**3**), 3,5-dibromocatechol (**4**), 4,5-dibromocatechol (**5**), 3,4,5-tribromocatechol (**6**), 3,4,6-tribromocatechol (**7**), and tetrabromocatechol (**8**) (Figure 2). We also selected six specific titanium complexes from this set of ligands for investigation: $[Ti(C_6H_4O_2)_3]^{2-}$ (**1a**), $[Ti(C_6H_3\text{-}4\text{-}BrO_2)_3]^{2-}$ (**3a**), $[Ti(C_6H_2\text{-}3,5\text{-}Br_2O_2)_3]^{2-}$ (**4a**), $[Ti(C_6H_2\text{-}4,5\text{-}Br_2O_2)_3]^{2-}$ (**5a**), $[Ti(C_6H\text{-}3,4,5\text{-}Br_3O_2)_3]^{2-}$ (**6a**), and $[Ti(C_6Br_4O_2)_3]^{2-}$ (**8a**) (Figure 2), all isolated as the $Me_2NH_2^+$ salts. We found that substituting $^{79/81}$Br in a ^{1}H spin system extends ^{1}H T_1 and T_2 by a factor of 4, depending on the pattern of the substitution. When complexed with Ti(IV), the ligand protons mimic the relaxation trends of the uncomplexed ligands. Yet, the relative variation is considerably more dramatic in the studied complexes, as ^{1}H T_1 and T_2 are enhanced by an order of magnitude depending on substitutional pattern. These data provide the first evidence of a synthetic design principle for modifying nuclear spin dynamics via substitutional patterning,

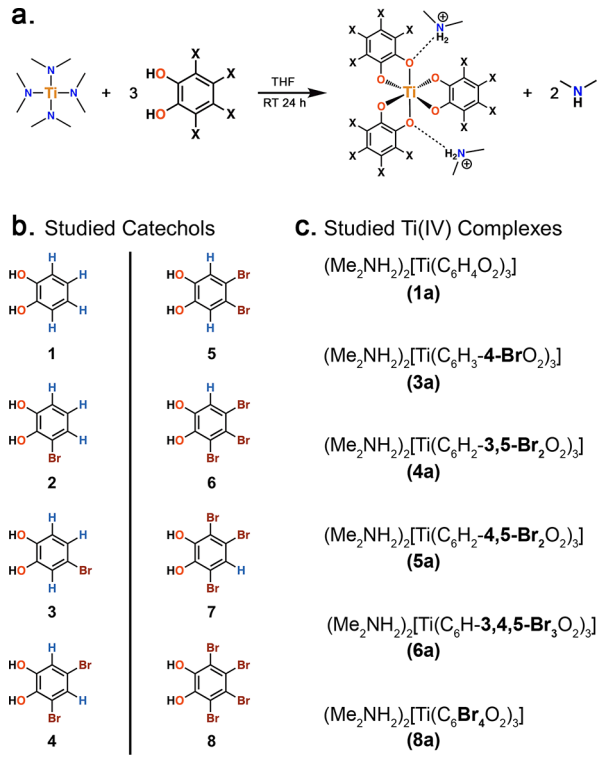

Figure 2. Synthetic scheme and complexes. (a) The general synthetic scheme to produce the titanium complexes is depicted. (b) The series of ten ligands used in this study. (c) Ligands **1**, **3**−**6**, and **8** were reacted to form six Ti(IV) coordination complexes following the scheme shown in (a).

and that coordination enhances the relative impact of the pattern design principle.

RESULTS

Isolation of the studied molecules proceeded with little difficulty. Indeed, many of the brominated catechols are available commercially (**1**, **2**, **3**, **8**) and all others were prepared via slight modifications of reported procedures (**4**−**7**).[25−27] Overnight reactions of 3.3 equiv of the catechols **1**, **3**, **4**, **5**, **6**, and **8** with 1 equiv of $Ti(NMe_2)_4$ in THF yielded dark red solutions containing **1a**, **3a**, **4a**, **5a**, **6a**, or **8a** (Figure 2), which can be isolated as orange powders. These reactions produce $Me_2NH_2^+$ counterions, suggesting that the Me_2N^- ligands of the Ti(IV) starting material $Ti(NMe_2)_4$ are deprotonating the catechol ligands during reaction progression. This same counterion formation by ligand deprotonation characterizes the synthesis of the analogous V(IV) complexes.[28,29]

Single-crystal X-ray diffraction of crystals resulting from the reactions of **1** and **5** with $Ti(NMe_2)_4$ reveals an octahedral geometry for the TiO_6 coordination environment (Figures 3 and S1, Tables S1−S3). These experiments reveal a general 3-to-1 ligand-to-metal stoichiometry and two $Me_2NH_2^+$ counterions. All other characterization data for the metal complexes match this general stoichiometry, though isolating high-quality single crystals of **3a**, **4a**, **6a**, and **8a** was significantly more challenging (see SI). Bond metrics taken from the obtained structures match literature expectations. For example, the average Ti−O distances in **1a** and **5a** are 1.9640(3) and 1.993(5) Å, respectively, close to those of known Ti-catecholate analogues.[30−32] Furthermore, C−O bond distances in the ligands are 1.345(8) Å which match those for the fully

https://dx.doi.org/10.1021/acs.inorgchem.0c00244
Inorg. Chem. XXXX, XXX, XXX−XXX

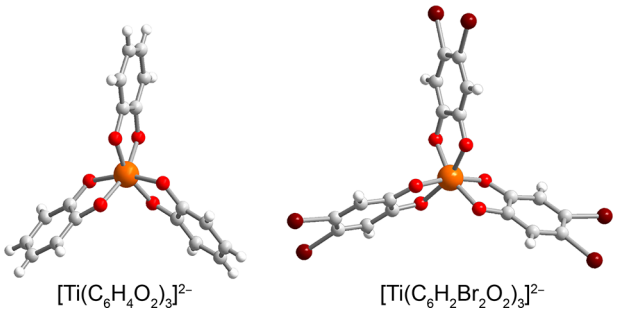

Figure 3. Molecular structures of $[Ti(C_6H_4O_2)_3]^{2-}$ (left) and $[Ti(C_6H_2Br_2O_2)_3]^{2-}$ (right), as determined in the crystal structures of **1a** and **5a**. Hydrogen bonding contacts with the $Me_2NH_2^+$ counterions are omitted for clarity. Orange, maroon, red, gray, and white spheres represent titanium, bromine, oxygen, carbon, and hydrogen atoms, respectively.

reduced catecholate, suggesting closed-shell ligands (as opposed to possible semiquinones, where C−O is 1.302(11) Å).[33] These data establish these molecules as closed-shell Ti(IV) complexes.

Proton NMR spectroscopy (400 MHz, 9.4 T) was applied to the ligands and complexes to locate and identify the chemical shifts of the nuclei of interest. All ligands and complexes depict ^{1}H peaks in the aromatic region (save for **8** and **8a**, which have only aromatic $^{79/81}$Br nuclear spins). Here, the peaks appear to be shifted downfield by proximity to either hydroxy or bromine groups. Furthermore, these peaks are split by *J*-coupling, where *J* is largest for 1,2-coupling between *ortho* protons (5.86−8.43 Hz) and decreasing as the protons are spaced apart on the catechol ring (2.05−3.57 Hz for 1,3-coupling between *meta* ^{1}Hs).[34] The 1,4-coupling strength between *para* ^{1}Hs was too small to observe for **1**, **3**, and **5** in our spectrometer. Peaks corresponding to OH groups for the free ligand show up from 7.76 to 9.22 ppm. The $Me_2NH_2^+$ counterions show peaks at 2.60 and 8.09−8.60 ppm for the $-CH_3$ and NH_2 protons, respectively, in the complexes. Upon complexation to Ti(IV), the catecholate ^{1}H aromatic peaks move slightly upfield but otherwise retain the same relative δ values and *J* couplings. The exception to the spectral similarity is complex **3a**, which exhibits rearranged peaks due to the removal of the shifting effect from the hydroxyl protons (Figures S3 and S9 in the SI).

Spin−lattice relaxation times were determined by standard ^{1}H NMR inversion−recovery experiments at room temperature (see Figures 4 and S2−S7 and the SI) for all ligands and complexes. These experiments proceeded with π pulses of 22 μs, and all catechol solutions were 200 mM in acetone-d_6. All Ti(IV) complexes were measured at 100 mM in DMSO-d_6 (solubility challenges precluded the use of acetone—see SI). NMR spectra were then collected following the initial π pulse, a variable-delay period, *T*, and a final $\pi/2$ pulse. For all ligands and complexes, the initial spectra following the π pulses are inverted, eventually recovering to the expected positive signal intensity. All recoveries were successfully fit with mono-exponential functions, suggesting that only a single relaxation process dominates for each peak. Importantly, the time scale of this recovery is peak-dependent (Figures 4 and S2−S8).

Our results show that, with minor exceptions, the substitution of Br atoms for H atoms engenders longer ^{1}H T_1 times (Table 1), based on four key observations. First, the shortest T_1 values are observed for protons that are adjacent to other protons. For example, the adjacent protons of **2** have T_1

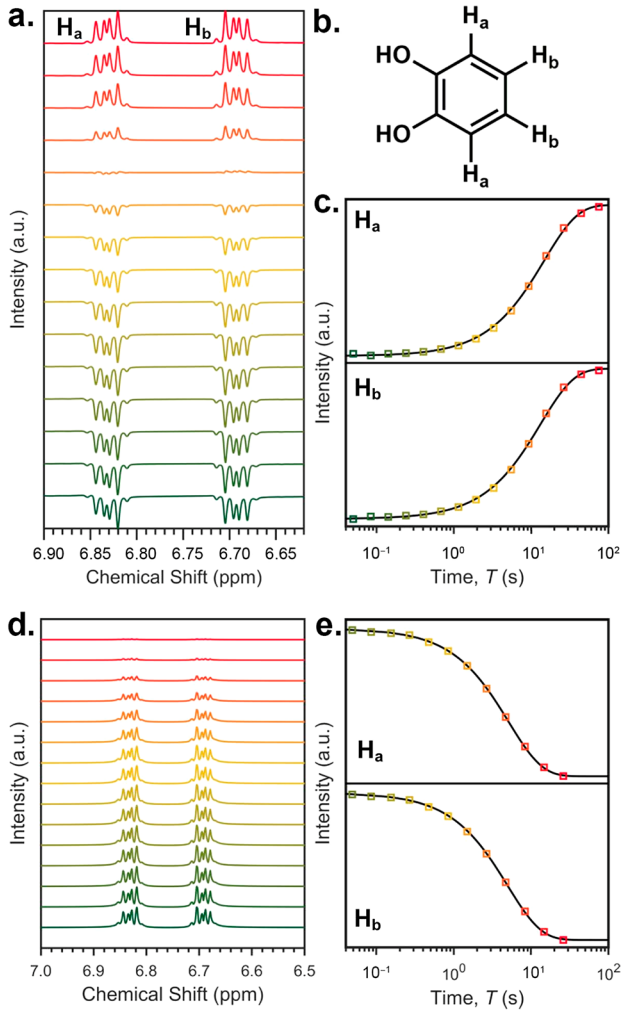

Figure 4. Example ^{1}H NMR analyses of a catechol molecule, here **1**. (a) Inversion−recovery spectra—the offset spectra represent different delay times between inversion and measurement, with the shortest delays at the bottom in green. (b) Depiction of ^{1}H peak assignment. (c) Peak intensity as a function of delay following inversion. The black line is a fit to an exponential recovery to yield T_1 for a given peak. (d) CPMG experimental results—the offset spectra represent different numbers of applied π pulses: the green spectrum at the bottom was collected with one π pulse and the red spectrum at the top was collected with 12 π pulses. (e) ^{1}H peak intensity versus total time after the $\pi/2$ pulse. The black line is a fit to an exponential decay to yield T_2 for the indicated peak.

times of 10.8(4) and 11.9(2) s, respectively, the shortest of **1**−**8**. This general trend holds true for the adjacent protons in **1** and **3**, which exhibit aromatic ^{1}H T_1 values only slightly longer compared to **2**, *ca.* 13−14 s. Second, the presence of a Br atom adjacent to a ^{1}H (versus another proton) appears to have a slight lengthening effect on T_1. Indeed, in **2**, the proton in the 4-position (which has one adjacent proton and one adjacent bromine) exhibits a slightly longer T_1 (17.9(4) s) than the other two protons of this ligand, which lack a neighboring Br atom (10−12 s). Third, T_1 is further lengthened when the Br atom isolates a given proton from other protons. For example, the ^{1}H in the 3-position of **3**, which is separated from the other protons, exhibits a relaxation time of 27(3) s, nearly twice as long as the proton in the corresponding position on **1**. Similarly, for **4** and **5**, which have no adjacent protons, the ^{1}H T_1 values are extended to 28−31 s. Finally, fourth, when only

https://dx.doi.org/10.1021/acs.inorgchem.0c00244
Inorg. Chem. XXXX, XXX, XXX−XXX

Table 1. Tabulated Aromatic ^{1}H Spin−Lattice Relaxation Times (T_1) Determined via Inversion Recovery Experiments[a,b,c]

	Ring Position			
Ligands	3	4	5	6
1	14.8(7)	13.3(6)	13.3(6)	14.8(7)
2		17.9(4)	10.8(4)	11.9(2)
3	27(3)		13.7(6)	13.4(7)
4		30(5)		31(5)
5	28(4)			28(4)
6				32(4)
7			43(5)	
	Ring Position			
Complexes	3	4	5	6
1a	1.32(2)	2.11(6)	2.11(6)	1.32(2)
3a	0.48(2)		0.74(8)	0.38(3)
4a		6.3(5)		6.8(3)
5a	6.0(5)			6.0(5)
6a				7.1(2)

[a]All T_1 values given in units of s. [b]There are no aromatic protons for **8** and **8a**, hence the omission. [c]T_1 values for OH groups and $Me_2NH_2^+$ counterions can be found in the SI.

one aromatic ^{1}H is present (as in the triply brominated **6** and **7**), T_1 can become even longer (32(4) and 43(5) s). In summary, these data demonstrate that T_1 can be varied by a factor of approximately four depending on the substitutional pattern.

The aromatic ^{1}H signals for the ligands display shorter *overall* T_1 values when coordinated to Ti(IV) (Figures 5, S9−S13, and Table 1). However, (and importantly), the same trends in ^{1}H T_1 values as a function of Br substitution patterns are seen for both the complexes and the lone ligands. For example, the adjacent protons in **3a** display the shortest T_1 values among the studied complexes, 0.48(2) and 0.38(3) s. In contrast, **4a**−**6a**, which have ^{1}H nuclear spins isolated from one another by Br atoms, exhibit T_1 values that are an order of magnitude greater (6.0(5) to 7.1(2) s).

Tests of the effects of substitutional pattering on ^{1}H T_2 were performed through application of Carr−Purcell−Meiboom−Gill (CPMG) experiments (Figures 4, 5, S2−S7, and S9−S12).[35,36] This experiment is similar to a Hahn-echo experiment; however, the time separating sequential π pulses is fixed, and the number of π pulses is varied, such that the total delay time between the initial pulse and the observed echo is the sum of repeated pulses and fixed delays. Application of the CPMG sequence to obtain T_2 removes field inhomogeneities as a potential impact on spin−spin relaxation—ensuring any determined trends are attributable to the studied complexes and not extrinsic effects. As with T_1, the time-dependent data set could be effectively modeled with a single exponential function, implying a single relaxation process is dominant. Critically, as with T_1, T_2 is peak-dependent.

The T_2 times of the aromatic protons in **1**−**8** broadly follow the trends seen in the T_1 data—greater degrees of bromination produce longer ^{1}H T_2 values (see Table 2). For example, the adjacent ligand ^{1}Hs on **1** were found to have T_2 parameters of approximately 5 s, which are the shortest of the series (second to **6**, see below). The singly brominated ligands **2** and **3** both have T_2 values that are larger than **1**, again consistent with T_1

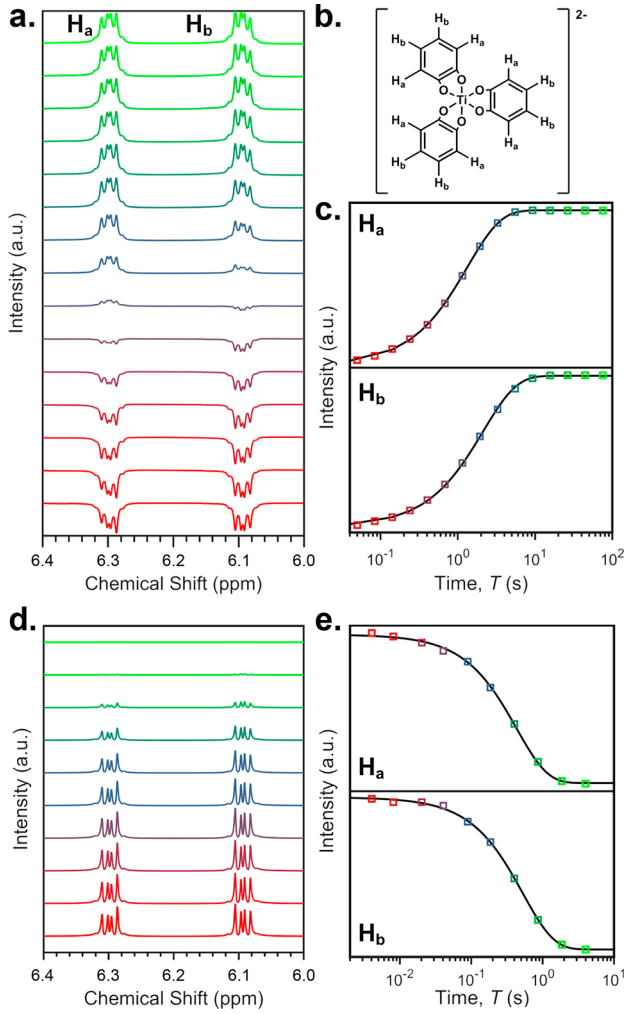

Figure 5. Example ^{1}H NMR analyses of a Ti(IV) catecholate complex molecule, here **1a**. (a) Inversion−recovery spectra—the offset spectra represent different delay times between inversion and measurement, with the shortest delays at the bottom in green. (b) Depiction of ^{1}H peak assignment. (c) Peak intensity as a function of delay following inversion. The black line is a fit to an exponential recovery to yield T_1 for a given peak. (d) CPMG experimental results—the offset spectra represent different numbers of applied π pulses: the red spectrum at the bottom was collected with one π pulse, and the fluorescent green spectrum at the top was collected with 10 π pulses. (e) ^{1}H peak intensity versus total time after the $\pi/2$ pulse. The black line is a fit to an exponential decay to yield T_2 for the indicated peak.

trends. Furthermore, protons in **3** and **5** that are isolated from the others by bromination show similar T_2 values. The doubly brominated **5**'s T_2 values fall within the range of **3**'s relaxation times. In contrast, the compositional isomer to **5**, with relatively closer ^{1}H spins, **4**, shows >60% relative lengthening of T_2. The two triply brominated ligands also display radically different T_2 values. **6** was found to have a T_2 of 4.30(4) s, shorter even than **1**. In contrast, **7** exhibits the longest T_2 of all of the ligands, 18(1) s, exceeding the T_1 of pyrocatechol. In summary, these data show substantial variation in T_2 with substitutional patterning that mimics the trends in T_1.

As with T_1, the spin−spin relaxation times of the aromatic ^{1}H ligand peaks all decrease upon complexation and generally follow the trends in T_1. For example, the ligand ^{1}Hs in **1a** exhibit the second-shortest T_2 values (~0.9 s), generally smaller than complexes where ^{1}H spins are separated by

https://dx.doi.org/10.1021/acs.inorgchem.0c00244
Inorg. Chem. XXXX, XXX, XXX−XXX

Table 2. Tabulated Aromatic ^{1}H Spin−Spin Relaxation Times (T_2) Determined with CPMG Pulse Sequences[a,b,c]

	Ring Position			
Ligands	3	4	5	6
1	5.1(2)	5.0(2)	5.0(2)	5.1(2)
2		6.3(6)	5.4(6)	6.0(3)
3	6.8(2)		6.5(2)	6.3(2)
4		10.9(9)		9.8(6)
5	6.5(3)			6.5(3)
6				4.30(4)
7			18(1)	
	Ring Position			
Complexes	3	4	5	6
1a	0.85(7)	0.9(3)	0.9(3)	0.85(7)
3a	0.22(1)		0.22(2)	0.23(1)
4a		3.42(4)		2.87(1)
5a	2.65(4)			2.65(4)
6a				2.88(5)

[a] T_2 values given in units of seconds. [b] There are no aromatic protons for **8** and **8a**, hence the omission. [c] T_2 values for OH groups and $Me_2NH_2^+$ counterions can be found in the SI.

bromines, which have T_2 parameters ranging from 2.65(4) s in **5a** to 3.42(4) s in **4a**. But, there are a few important exceptions in the correlation to T_1. For example, the aromatic ^{1}H peaks of **3a** have the shortest T_2 values of the studied complexes (0.22(1) to 0.23(1)) s, despite having a Br atom. Second, the complex with triply brominated ligands, **6a**, has a T_2 that is within the range of the other complexes (2.88(5) s), when the ligand for this complex, **6**, has the longest T_2 of all the ligands. These few exceptions point to more complicated relaxation dynamics in the complexes than dipole effects from only the ligand shell, in contrast to the pure ligands.

DISCUSSION

The collected NMR data paint a rich picture of the ^{1}H nuclear spin dynamics within the studied species and reveal a path toward bespoke nuclear magnetization dynamics in the ligand shell. The results further point toward dipole-driven relaxation processes as the synthetically tunable feature. Here, whenever a proton is replaced by a $^{79/81}$Br nucleus in a given ligand, the strong ^{1}H···^{1}H interaction of that proton with neighboring ones is replaced by the relatively weaker coupling to the bromine (as $^{79/81}$Br have a smaller magnetic moment). This switch results in the general lengthening of both T_1 and T_2 for the ^{1}H spins with increasing bromine content across the series of tested ligands. In the following analyses, note that we ignore the impact of potential ^{13}C nuclear spins in the ligands, as this $I = {}^1/_2$ isotope is only 1% naturally abundant.[23]

We tested the correlation between ^{1}H relaxation times and dipolar interactions to better quantitate the T_1/T_2 trends for the studied species. For this test, we computed the ^{1}H dipole-driven spin−lattice (T_1^{DD}) and spin−spin (T_2^{DD}) relaxation times which stem from a sum of dipole−dipole interactions with all surrounding magnetic nuclei and a rotational correlation time (Figure 6), τ_c[37−39] (see SI for detailed equations and interpretation). Comparison of the experimental T_1 and T_2 values with the computed values is shown in Figures 6 and S14. Relatively good linear correlations are seen for T_1 (R^2 = 0.91), when the τ_c values for all protonated catechol ligands (**1**−**7**) are assumed to be 9 ps, as is typical of small

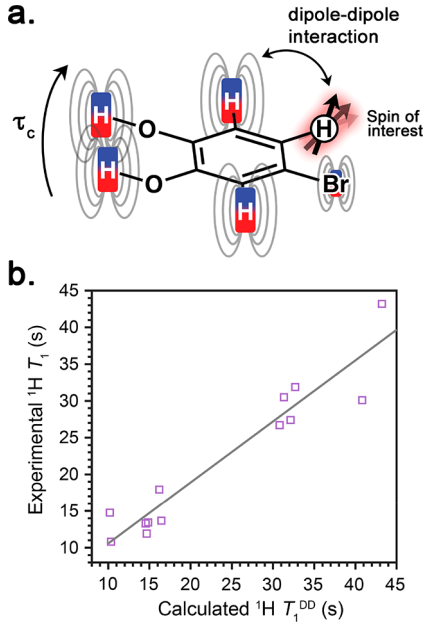

Figure 6. (a) Each proton in the ligand experiences dipolar interactions with other nuclear spins in its vicinity. Rotation of the molecule (on a time scale called the correlation time, τ_c) impacts the T_1 and T_2 of a spin of interest through dipolar coupling between the spin of interest and other nuclear spins in the environment. (b) Comparison of the experimental ^{1}H ligand T_1 relaxation times with the computed T_1 considering only dipole−dipole interactions, T_1^{DD} and assuming the same τ_c, 9 ps, for **1**−**7** (**8** has no protons on the ligand shell). The high correlation between the two data sets (gray line, R^2 = 0.91) suggests that spin−lattice relaxation in these systems is governed predominantly by dipole−dipole effects between a given proton and its nearest neighbors.

molecules.[36] Low correlation with T_2 is observed, however, which may stem from the CPMG sequence, as well as the fundamental assumption of the same τ_c for all ligands (see SI). When the experimental T_1 is set as T_1^{DD}, numerical solutions for τ_c are obtained. The determined τ_c values via this method range from ca. 6 to 12 ps, well within the bounds of what is reasonable for small organic molecules (Table S5).[40−42] This slight variation in τ_c for protons in ligands/complexes with nearly the same chemical composition likely stems from differences in mass distributions (owing to the heavy Br atoms), which will affect motion in solution.[43,44]

Similar comparison of experimental ^{1}H T_1/T_2 with T_1^{DD}/T_2^{DD} for the metal complexes is of lower quality, and τ_c cannot be extracted in some cases, unlike the ligands (Table S5). When τ_c times can be extracted, they are categorically longer than those for the ligands, consistent with the picture of decreased relaxation times for longer τ_c values in small molecules. Furthermore, the general trend in spin dynamics from the ligands carries over to the metal complexes: when protons are separated by Br atoms, ^{1}H spin relaxation becomes slower. On this basis, we conclude that the general mechanism of ^{1}H spin relaxation in the ligands is likely also present in the metal complexes. Precise modeling of T_1 and T_2 here would require accounting for intramolecular association (as is known for catechol),[45] and ligand-to-ligand and ligand-to-$H_2NMe_2^+$ interactions. We posit that the impact of the counterion is relatively weak. Otherwise, T_1 and T_2 would be smaller for every ^{1}H in the 3 and 6 positions of the studied complexes, as these positions are closest to the hydrogen-bonded counterion.

https://dx.doi.org/10.1021/acs.inorgchem.0c00244
Inorg. Chem. XXXX, XXX, XXX−XXX

In this light, **3a** and **4a** are important, as the 3- and 6-position protons here have T_1 or T_2 values that are comparable or longer than protons in the 4 and 5 positions. Other factors that prevent perfect correlation include lengthening of T_2 via the quantum zeno effect[46] and other relaxation processes, e.g. scalar or chemical shift anisotropy processes, though they are relatively minor contributions to ^{1}H T_1 and T_2 compared to the dipolar mechanism.[36,37] Future studies by us will test many of the foregoing ideas, especially counterion effects.

As one final point, the impact of the bromination in the ligands and complexes could be linked to manipulation of τ_c, not control of dipolar interactions. However, the trends in τ_c do not follow the trends in T_1 or T_2. For example, the longest T_1 observed in the ligands is 43(5) s for **7**, yet this ligand exhibits a correlation time (τ_c = 8.8 ps) within the range of all of the other ligands (6.1 to 12 ps). Furthermore, the shortest τ_c times for the metal complexes were found for **1a**, yet this complex does not display the shortest T_1 and T_2 for the studied complexes. We take this observation and the correspondence of the trends in the ligands and complexes as the final evidence that the operative mechanism by which spin patterning affects relaxation is through dipolar interactions.

It is noteworthy that comparison of the foregoing results with trends in ^{1}H T_1 and T_2 for other ligand systems is nearly impossible, since explicit studies targeting ligand nuclear spin dynamics via synthetic design are, to the best of our knowledge, unrepresented in the literature. We can, however, compare our results with studies of proton spin dynamics in simple haloalkanes. Here, our results agree with these previous studies, which found increasing T_1 and T_2 with increasing degree of halogenation via weakening the overall ^{1}H···^{1}H dipolar interactions.[38,39] These studies found relative variation in T_1 of up to a factor of 16, slightly lower than we found for our metal complexes, but beyond what we observed for the isolated ligands. This benchmark underscores the high tunability in the nuclear spin-dynamics of ligands (given the discovery of the right design strategies) and also the importance of coordination.

OUTLOOK

The dynamics of nuclear spins close to metal-based electronic spins are profoundly important for determining electronic spin relaxation times. Yet, understanding how to control those nuclear spin dynamics to precisely direct the magnetic properties of metal ions is a significant fundamental challenge. This paper represents an important step toward that goal by clearly demonstrating (1) the possibility of controlling the dynamics of ligand-based nuclei via patterning and (2) that design principles for isolated ligands can be translated directly to metal complexes (if that metal is closed-shell). Importantly these results also demonstrate that the design principles for T_1 and T_2 are enhanced upon coordination, suggesting that future studies of nuclear spin dynamics in the ligand shell will yield significant fundamental insight. An enormous body of knowledge targets understanding how coordination geometry, symmetry, donor atom strength, etc. affect electron spin relaxation in metal complexes (e.g., refs 47−53). But, to the best of our knowledge, none has tested direct synthetic manipulation of the nuclear spin dynamics within the ligand shell as a potential design parameter for lengthening electron spin relaxation. We thus hope that this work and others from our group will inspire future studies in this undoubtedly rich area.

ASSOCIATED CONTENT

Supporting Information

The Supporting Information is available free of charge at https://pubs.acs.org/doi/10.1021/acs.inorgchem.0c00244.

Full experimental details, including sample preparation and analyses. Additional magnetic resonance characterization. (PDF)

Accession Codes

CCDC 1979699−1979700 contain the supplementary crystallographic data for this paper. These data can be obtained free of charge via www.ccdc.cam.ac.uk/data_request/cif, or by emailing data_request@ccdc.cam.ac.uk, or by contacting The Cambridge Crystallographic Data Centre, 12 Union Road, Cambridge CB2 1EZ, UK; fax: +44 1223 336033.

AUTHOR INFORMATION

Corresponding Author

Joseph M. Zadrozny − *Department of Chemistry, Colorado State University, Fort Collins, Colorado 80523, United States;* orcid.org/0000-0002-1309-6545; Email: joe.zadrozny@colostate.edu

Authors

Spencer H. Johnson − *Department of Chemistry, Colorado State University, Fort Collins, Colorado 80523, United States*

Cassidy E. Jackson − *Department of Chemistry, Colorado State University, Fort Collins, Colorado 80523, United States*

Complete contact information is available at: https://pubs.acs.org/10.1021/acs.inorgchem.0c00244

Author Contributions

S.H.J. and C.E.J. executed the syntheses and characterization. S.H.J., C.E.J., and J.M.Z. conducted spectroscopic analyses and data interpretation. All authors were involved in assembling the manuscript.

Notes

The authors declare no competing financial interest.

ACKNOWLEDGMENTS

We thank Joseph DiVerdi, Richard Eykholt, Buzz Walters, and Matt Phelan for fruitful conversation and graphical assistance. This research was performed with the support of Colorado State University (CSU) and the National Science Foundation (CHE-1836537). S.H.J. acknowledges the National Institutes of Health through the Northern Colorado Bridges to Baccalaureate Program (1R25GM115300-4), the CSU Energy Institute, and the Colorado Chapter of the ARCS Foundation for support at different stages of this study. C.E.J. was supported in part by a CSU Program of Research and Scholarly Excellence fellowship through the Center of Advanced Magnetics. Nuclear magnetic resonance experiments and standard molecular characterization were performed at the CSU Central Instrument Facility, which is supported by an NIH-SIG award (1S10OD021814-01) and the CSU-CORES Program.

REFERENCES

(1) Schirhagl, R.; Chang, K.; Loretz, M.; Degen, C. L. Nitrogen-Vacancy Centers in Diamond: Nanoscale Sensors for Physics and Biology. *Annu. Rev. Phys. Chem.* **2014**, *65* (1), 83−105.

(2) Lovchinsky, I.; Sushkov, A. O.; Urbach, E.; de Leon, N. P.; Choi, S.; De Greve, K.; Evans, R.; Gertner, R.; Bersin, E.; Müller, C.;

McGuinness, L.; Jelezko, F.; Walsworth, R. L.; Park, H.; Lukin, M. D. Nuclear Magnetic Resonance Detection and Spectroscopy of Single Proteins Using Quantum Logic. *Science* **2016**, *351* (6275), 836−841.
(3) Stolze, J.; Dieter, S. *Quantum Computing: A Short Course from Theory to Experiment*; Wiley-VCH, Weinheim, 2004.
(4) Nielsen, M. A.; Chuang, I. L. *Quantum Computation and Quantum Information*; Cambridge University Press, Cambridge, 2011.
(5) Griffin, R.; Prisner, T. High Field Dynamic Nuclear Polarization−the Renaissance. *Phys. Chem. Chem. Phys.* **2010**, *12*, 5737−5740.
(6) Winpenny, R. E. P. Quantum Information Processing Using Molecular Nanomagnets as Qubits. *Angew. Chem., Int. Ed.* **2008**, *47* (42), 7992−7994.
(7) Ardavan, A.; Rival, O.; Morton, J. J. L.; Blundell, S. J.; Tyryshkin, A. M.; Timco, G. A.; Winpenny, R. E. P. Will Spin-Relaxation Times in Molecular Magnets Permit Quantum Information Processing? *Phys. Rev. Lett.* **2007**, *98* (5), 1−4.
(8) Bader, K.; Winkler, M.; Van Slageren, J. Tuning of Molecular Qubits: Very Long Coherence and Spin-Lattice Relaxation Times. *Chem. Commun.* **2016**, *52* (18), 3623−3626.
(9) Lehmann, J.; Gaita-Ariño, A.; Coronado, E.; Loss, D. Quantum Computing with Molecular Spin Systems. *J. Mater. Chem.* **2009**, *19* (12), 1672−1677.
(10) Aromi, G.; Aguilà, D.; Gamez, P.; Luis, F.; Roubeau, O. Design of magnetic coordination complexes for quantum computing. *Chem. Soc. Rev.* **2012**, *41*, 537−546.
(11) Atzori, M.; Sessoli, R. The Second Quantum Revolution: Role and Challenges of Molecular Chemistry. *J. Am. Chem. Soc.* **2019**, *141* (29), 11339−11352.
(12) Zadrozny, J. M.; Niklas, J.; Poluektov, O. G.; Freedman, D. E. Millisecond Coherence Time in a Tunable Molecular Electronic Spin Qubit. *ACS Cent. Sci.* **2015**, *1* (9), 488−492.
(13) Yu, C.-J.; Graham, M. J.; Zadrozny, J. M.; Niklas, J.; Krzyaniak, M.; Wasielewski, M. R.; Poluektov, O. G.; Freedman, D. E. Long Coherence Times in Nuclear Spin-Free Vanadyl Qubits. *J. Am. Chem. Soc.* **2016**, *138*, 14678−14685.
(14) Eaton, S. S.; Eaton, G. R. In *Biological Magnetic Resonance*; Berliner, L. J., Eaton, S. S., Eaton, G. R., Eds.; Kluwer academic/Plenum publishers: New York, 2002; Vol. *19*, pp 29−154.
(15) Bloembergen, N.; Purcell, E. M.; Pound, R. V. Relaxation effects in nuclear magnetic resonance absorption. *Phys. Rev.* **1948**, *73*, 679−712.
(16) Solomon, I. Relaxation processes in a system of two spins. *Phys. Rev.* **1955**, *99*, 559−565.
(17) Levitt, M. H. *Spin Dynamics*, 2nd ed.; John Wiley & Sons, Ltd: West Sussex, 2008.
(18) Carrington, A.; McLachlan, A. D. *Introduction to Magnetic Resonance*, 2nd ed.; Harper & Row: New York, 1969.
(19) Jackson, C. E.; Lin, C.-Y.; Johnson, S. H.; van Tol, J.; Zadrozny, J. M. Nuclear-spin-pattern control of electron-spin dynamics in a series of V(IV) complexes. *Chem. Sci.* **2019**, *10*, 8447−8454.
(20) Falk, A. L.; Buckley, B. B.; Calusine, G.; Koehl, W. F.; Dobrovitski, V. V.; Politi, A.; Zorman, C. A.; Feng, P. X.-L.; Awschalom, D. D. Polytype control of spin qubits in silicon carbide. *Nat. Commun.* **2013**, *4*, 1819.
(21) Weber, J. R.; Koehl, W. F.; Varley, J. B.; Janotti, A.; Buckley, B. B.; Van de Walle, C. G.; Awschalom, D. D. Defects in SiC for quantum computing. *J. Appl. Phys.* **2011**, *109*, 102417.
(22) Koehl, W. F.; Buckley, B. B.; Heremans, F. J.; Calusine, G.; Awschalom, D. D. Room temperature coherent control of defect spin qubits in silicon carbide. *Nature* **2011**, *479*, 84−87.
(23) *CRC Handbook of Chemistry and Physics*, 99th ed.; Rumble, J., Ed.; CRC Press, 2018.
(24) Chaffin, J. H.; Hubbard, P. S. Nuclear magnetic relaxation and Overhauser effectsin liquid CHF_3. *J. Chem. Phys.* **1967**, *46*, 1511−1520.
(25) Dakin, H. D. Synthesis of Catechol. *Org. Synth.* **1923**, *3*, 28.
(26) Kohn, M. Bromination of Catechol. *J. Am. Chem. Soc.* **1951**, *73* (1), 480.
(27) Kohn, M.; Steiner, L. The Reduction of Bromo Derivatives of Catechol, Resorcinol, and Pyrogallol. *J. Org. Chem.* **1947**, *12* (1), 30−33.
(28) Lin, C. Y.; Ngendahimana, T.; Eaton, G. R.; Eaton, S. S.; Zadrozny, J. M. Counterion Influence on Dynamic Spin Properties in a V(IV) Complex. *Chem. Sci.* **2019**, *10*, 548−555.
(29) Cooper, S. R.; Koh, Y. B.; Raymond, K. N. Synthetic, Structural, and Physical Studies of Bis(Triethylammonium) Tris-(Catecholato)Vanadate(IV), Potassium Bis(Catecholato)-Oxovanadate(IV), and Potassium Tris(Catecholato)Vanadate(III). *J. Am. Chem. Soc.* **1982**, *104* (19), 5092−5102.
(30) Assi, H.; Haouas, M.; Mouchaham, G.; Martineau-Corcos, C.; Allain, C.; Clavier, G.; Guillou, N.; Serre, C.; Devic, T. $MgTi(Cat)_3$, a Promising Precursor for the Preparation of Ti−MOFs? *Polyhedron* **2018**, *156*, 111−115.
(31) Borgias, B. A.; Cooper, S. R.; Koh, Y. B.; Raymond, K. N. Synthetic, Structural, and Physical Studies of Titanium Complexes of Catechol and 3,5-Di-Tert-Butylcatechol. *Inorg. Chem.* **1984**, *23* (8), 1009−1016.
(32) Dong, G.-L.; Wang, L.; Fang, W.-H.; Zhang, L. Hydrothermal synthesis, structures and visible light harvest of three titanium complexes. *Inorg. Chem. Commun.* **2018**, *93*, 61−64.
(33) Brown, S. N. Metrical Oxidation States of 2-Amidophenoxide and Catecholate Ligands: Structural Signatures of Metal−Ligand π Bonding in Potentially Noninnocent Ligands. *Inorg. Chem.* **2012**, *51*, 1251−1260.
(34) Silverstein, R. M.; Webster, F. X.; Kiemle, D. J. *Spectrometric Identification of Organic Compounds*, 7th ed.; John Wiley & Sons: Hoboken, 2005.
(35) Carr, H. Y.; Purcell, E. M. Effects of Diffusion on Free Precession in Nuclear Magnetic Resonance Experiments. *Phys. Rev.* **1954**, *94* (3), 630−638.
(36) Meiboom, S.; Gill, D. Modified spin-echo method for measuring nuclear relaxation times. *Rev. Sci. Instrum.* **1958**, *29*, 688−691.
(37) Sudmeier, J. L.; Anderson, S. E.; Frye, J. S. Calculation of Nuclear Spin Relaxation Times. *Concepts Magn. Reson.* **1990**, *2* (4), 197−212.
(38) Farrar, T. C.; Becker, E. D. Relaxation Mechanisms. *Pulse and Fourier Transform NMR* **1971**, 46−65.
(39) Abragam, A. Thermal Relaxation in Liquids and Gases. In *The Principles of Nuclear Magnetism*; The Clarendon Press: Oxford, 1961; pp 264−353.
(40) Miller, C. R.; Gordon, S. L. Proton Spin Relaxation in the Chloroethanes. *J. Chem. Phys.* **1970**, *53* (9), 3531−3538.
(41) Brown, P. M.; Krishna, N. R.; Gordon, S. L. Proton Spin Relaxation in the Halomethanes. *J. Magn. Reson.* **1975**, *20* (No. 20), 540−543.
(42) Lee, D. H.; McClung, R. E. D. Nuclear Relaxation and Molecular Motion of 1,3,5-Trifluorobenzene-d_3 in Liquid Solutions. *Chem. Phys.* **1987**, *116* (1), 101−111.
(43) Steele, W. A. Molecular Reorientation in Liquids. II. Angular Autocorrelation Functions. *J. Chem. Phys.* **1963**, *38* (10), 2411−2418.
(44) Díez, E.; Bermejo, F. J.; Guilleme, J. Molecular Reorientation from NMR Relaxation Times in Planar Molecules. *J. Chem. Phys.* **1985**, *83* (1), 58−69.
(45) Kuhn, L. The Hydrogen Bond. I. Intra- and Intermolecular hydrogen bonds in alcohols. *J. Am. Chem. Soc.* **1952**, *74*, 2492−2499.
(46) Xiao, L.; Jones, J. A. NMR Analogues of the quantum zeno effect. *Phys. Lett. A* **2006**, *359*, 424−427.
(47) Sessoli, R.; Powell, A. K. Strategies toward single molecule magnets based on lanthanide ions. *Coord. Chem. Rev.* **2009**, *253*, 2328−2341.
(48) Craig, G. A.; Murrie, M. 3d single-ion magnets. *Chem. Soc. Rev.* **2015**, *44*, 2135−2147.
(49) Liddle, S. T.; van Slageren, J. Improving f-element single molecule magnets. *Chem. Soc. Rev.* **2015**, *44*, 6655−6669.

https://dx.doi.org/10.1021/acs.inorgchem.0c00244
Inorg. Chem. XXXX, XXX, XXX−XXX

(50) Frost, J. M.; Harriman, K. L. M.; Murugesu, M. The rise of 3-d single-ion magnets in molecular magnetism: toward materials from molecules? *Chem. Sci.* **2016**, *7*, 2470−2491.
(51) Meng, Y.-S.; Jiang, S.-D.; Wang, B.-W.; Gao, S. Understanding the magnetic anisotropy toward single-ion magnets. *Acc. Chem. Res.* **2016**, *49*, 2381−2389.
(52) Rinehart, J. D.; Long, J. R. Exploiting single-ion anisotropy in the design of f-element single-molecule magnets. *Chem. Sci.* **2011**, *2*, 2078−2085.
(53) Feng, M.; Tong, M.-L. Single ion magnets from 3d to 5f: developments and strategies. *Chem. - Eur. J.* **2018**, *24*, 7574−7594.

https://dx.doi.org/10.1021/acs.inorgchem.0c00244
Inorg. Chem. XXXX, XXX, XXX−XXX